BULLETIN OF THE EARTHQUAKE
RESEARCH INSTITUTE
Vol. 48 (1970), pp. 811-833

44. *Anomalous Underground Structure in the Matsushiro Earthquake Swarm Area as Derived from a Fan Shooting Technique.*

By

Hiroshi OKADA, Sadaomi SUZUKI,
Faculty of Science, Hokkaido University
and
Shuzo ASANO,
Earthquake Research Institute.

(Read Feb. 24 and May 26, 1970.—Received July 7, 1970.)

Abstract

During explosion seismic studies in the Matsushiro Earthquake Swarm Area the seismic waves from shot B-IV were observed at the observation sites in profile A. The travel time studies as well as the frequency studies of the initial portion of P waves show clearly the coincidence between the region with a low interval velocity as well as with high attenuation, and the seismically most active region.

1. Introduction

The detailed explosion seismic study of the Matsushiro Earthquake Swarm area conducted in 1967 revealed an anomalous underground structure corresponding to the seismically most active region (Asano *et al.*, 1969a,b). The results of this study showed clearly the significance of the detailed investigation of the crustal structure in the study of seismic activity.

Most of the earthquakes in this area have occurred at very shallow depths as reported earlier (Hagiwara, T. and T. Iwata, 1968). Especially in the seismically most active area the focal depths of earthquakes are smallest, being only about 1 km below the mean sea level. Such anomalous features as a hidden fault infered from surface fissures (Nakamura, K. and Y. Tsuneishi, 1967), a rapid uplift (Tsubokawa, I. *et al.*, 1967), a rapid change in the inclination of earth's surface (Hagiwara, T. *et al.*, 1966), a large contraction (Kasahara, K. *et al.*, 1966a, 1966b, 1967), etc. were also observed in the same area. Therefore, it might be interesting to elaborate the underground structure in this area and to clarify

its relation to the anomalous events mentioned above. From this point of view, it is quite important to search for a direct evidence of the existence of an anomalous structure in the hypocentral region in comparison with the underground structures in the surrounding regions, no matter whether this anomalous structure may be one of the main causes or a result of earthquake occurrence.

In the case of the explosion seismic experiment in 1967, a "fan shooting technique" was applied tentatively to discover an anomalous structure in the hypocentral region. As is well known, this technique is powerful to locate a local anomaly of the underground structure and is used sometimes in seismic prospecting. However, in the present case, the situation is quite different from that in the seismic prospecting, i.e. the surveyed area is much larger and its geology is much more complicated than in usual seismic prospecting. In spite of these different situations, an anomalous decrease of wave velocity as well as an anomalous dissipation of waves were derived in the hypocentral region from the data obtained with the fan shooting technique.

2. Shot point and observation sites

The location of the shot point and the observation sites is shown in Fig. 1. Dynamite of 234.0 kg was fired at one of shot points, B-IV, in profile B. Corresponding observations were made at sites in profile A. The range of azimuths of the observation sites from the shot point is about 114.°3 from N 14.°3 E to S 80°.0 W. The distance from the shot point to the nearest observation site, D_9-c, is 19.65 km. The epicentral distance to the most northern observation site, D_1-a, is 46.54 km and that to the observation site, D_{14}-e at the southern end of profile A is 29.29 km. Epicentral distances, azimuths and travel times for each observation site are given in Table 1.

The epicentral area of the swarm earthquakes is almost covered by the triangle with apexes B-IV, D_1, and D_{14}. To locate clearly the paths of seismic waves in the Matsushiro Earthquake Swarm area, the released seismic energy ratio is shown by contours in Fig. 1. The released seismic energy ratio is the ratio of the released seismic energy in the period from August 1965 to May 1968 to the possible maximum strain energy to be stored within a fixed volume up to the depth 5 km, both of which being derived by Ichikawa (1969). Therefore a large number in this figure implies large seismic activity in the area concerned.

As seen in Fig. 1, some of the lines connecting each observation site with the shot point cut the contours of the released seismic energy in various ways and some pass the area without any seismic activity as

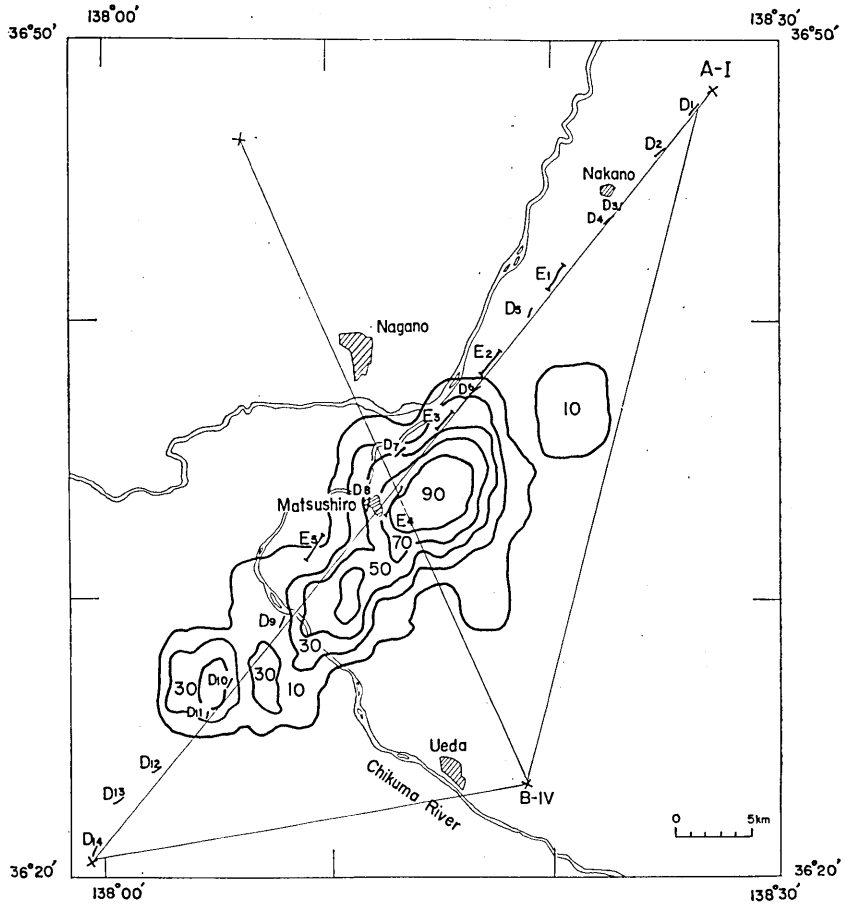

Fig. 1. Observation sites for the shot at B-IV. Contours show released seismic energy ratio. Number denotes the released seismic energy ratio in %. The line NE-SW is profile A and the line NW-SE is profile B for the explosion seismic studies.

Table 1. Distance of observation points from shot point B-IV, azimuth measured clockwise from north at shot point and travel time data

Observation Point		Geophone*	Δ (km)	Azimuth (°)	Class**	Travel Time (sec)
D_2	a	4 V	43.170	12.146	C	(8.16)
	b	1 V	43.060	11.887	B	8.106
	c	4 V	42.685	11.444	B	8.067
D_3	a	1 V	39.216	9.154	B	7.338
	b	4 V	38.937	9.170	B	7.294
	c	2 V	38.577	8.744	B	7.283
D_4	a	4 V	38.320	8.425	B	7.288
	b	2 V	38.084	8.191	B	7.278
	c	4 V	37.798	7.899	C	7.18

(to be continued)

Table 1. (continued)

Observation Point		Geophone*	Δ (km)	Azimuth (°)	Class**	Travel Time (sec)
D_5	a	1 V	31.672	0.909	A	6.353
	b	1 V	31.415	0.634	A	6.297
	c	1 V	31.070	359.621	B	6.246
D_6	a	1 V	26.859	353.295	B	5.386
	b	1 V	26.544	352.190	B	5.436
	c	1 V	26.350	351.412	B	5.393
D_7	a	4 V	23.985	340.639	B	4.948
	b	1 V	23.681	340.383	A	4.868
	c	4 V	23.515	338.529	A	4.800
D_8	a	4 V	21.536	330.940	C	4.46
	b	1 V	21.170	330.498	C	4.40
	c	4 V	21.024	329.857	C	4.37
	b′	4 V	21.080	330.197	A	4.371
	b	1 $H_{//}$	21.170	330.498	B	4.390
	b	1 $H_{\angle R}$	21.170	330.498	C	4.39
D_9	b	1 V	19.724	303.897	C	4.16
	c	1 V	19.647	302.886	C	4.20
D_{10}	a	4 V	20.934	289.733	B	4.488
	b	1 V	20.924	288.907	A	4.481
	c	4 V	21.179	287.977	B	4.539
D_{11}	a	4 V	21.761	283.274	A	4.661
	b	1 V	21.729	282.574	A	4.624
	c	4 V	21.748	282.025	C	4.62
D_{12}	a	4 V	24.234	272.835	B	5.090
	b	1 V	24.564	272.229	B	5.127
	c	4 V	24.853	271.745	B	5.207
D_{13}	a	4 V	26.655	268.108	B	5.545
	b	1 V	26.991	267.874	B	5.638
	c	4 V	27.127	267.440	B	5.724
D_{14}	a	4 V	28.872	261.608	C	6.10
	c	1 V	28.994	261.089	C	6.15
	d	4 V	29.087	260.631	C	6.17
	e	4 V	29.157	260.455	C	6.20
E_3	2	4.5V	25.370	348.577	B	5.186
	3	4.5V	25.299	348.361	B	5.193
	4	4.5V	25.254	348.234	C	5.17
	5	4.5V	25.194	348.021	B	5.134
	6	4.5V	25.130	347.858	B	5.125
	7	4.5V	25.081	347.663	B	5.116
	8	4.5V	25.011	347.447	B	5.125
	9	4.5V	24.959	347.273	C	5.13
	10	4.5V	24.900	347.072	C	5.14
	11	4.5V	24.825	346.911	C	(5.11)
	12	4.5V	24.773	346.752	C	(5.11)
	13	4.5V	24.718	346.396	B	5.100
	14	4.5V	24.661	346.283	B	5.094
	16	4.5V	24.590	345.878	A	5.063
	17	4.5V	24.474	345.681	A	5.050
	18	4.5V	24.392	345.496	B	5.041
	19	4.5V	24.346	345.291	B	5.022
	20	4.5V	24.251	345.109	B	5.019
	22	4.5V	24.142	344.754	B	4.978
	23	4.5V	24.076	344.535	B	4.959
	24	4.5V	24.020	344.321	B	4.941

* 4V means that the geophone used was of vertical type with a natural frequency of 4 hz. $1H_{//}$ means that the geophone of horizontal type with a natural frequency of 1 hz is set so as to register the longitudinal component of horizontal ground movement and $1H_{\angle R}$, to register the transversal component.

** Refer to Asano *et al.*, 1969a.

far as the felt earthquakes are concerned. Since the underground structures are unknown in the region except for that in profiles A and B, it is impossible to derive exact wave paths from the shot point to each observation site. However, in this paper the lines connecting each observation site with the shot point are assumed to be the actual wave paths by taking the accuracy of the underground structure derived in profiles A and B into account. It should be remembered that among the wave paths those to the observation sites D_6, E_3, D_7, and D_8 cross the seismically most active regions. The wave paths to the observation sites D_{10}, D_{11}, D_{12}, D_{13}, and D_{14} include the area with fairly thick sedimentary layers in the geological map (Nagano-ken Chigakukai, 1962). The area north of Chikuma River is almost included in the Central Belt of Uplift.

3. Anomaly in travel times

Most of the seismograms obtained with the tape recorders give clear onsets as shown in Fig. 2. The quality of the seismograms obtained at D_1, E_1, E_2, E_4, and E_5 being not so good because of a poor signal to noise ratio, these seismograms are not used in the present analysis. The seismogram at E_3' in profile B from shot B-IV (Asano *et al.*, 1969a) is also used for the discussion since its quality as well as the location of the observation site are good enough. The first arrivals of P waves at each observation site are those of the refracted waves traveling through the top of the layer with a velocity of 6.0 km/s, referring to the underground structures in profiles A and B or to the travel time curves (Asano *et al*, 1969a). In order to study the velocity anomaly within this layer it is necessary to subtract the travel time due to the surface layer (the velocity: 1.6-2.3 km/s) as well as the first layer (the velocity: 3.3-4.75 km/s) from the observed travel times. That is, the delay times due to the surface and the first layers for each observation site and for shot point B-IV should be subtracted. It is assumed that the underground structure around each observation site is the same in profile A for shot B-IV with that already obtained (Asano *et al*, 1969b) since there are no direct measurements available.

The underground structure around shot point B-IV is assumed to be the same with that obtained in profile B. Then $T-T'$ from profile A can be used as the delay time for each observation site, where T stands for the observed travel time and T', for the travel time derived by the method of differences (Asano *et al*, 1969b). Also $T-T'$ at shot point B-IV is obtained by extending the T' curve in profile B to shot point B-IV. The subtraction of the delay time thus obtained, from the ob-

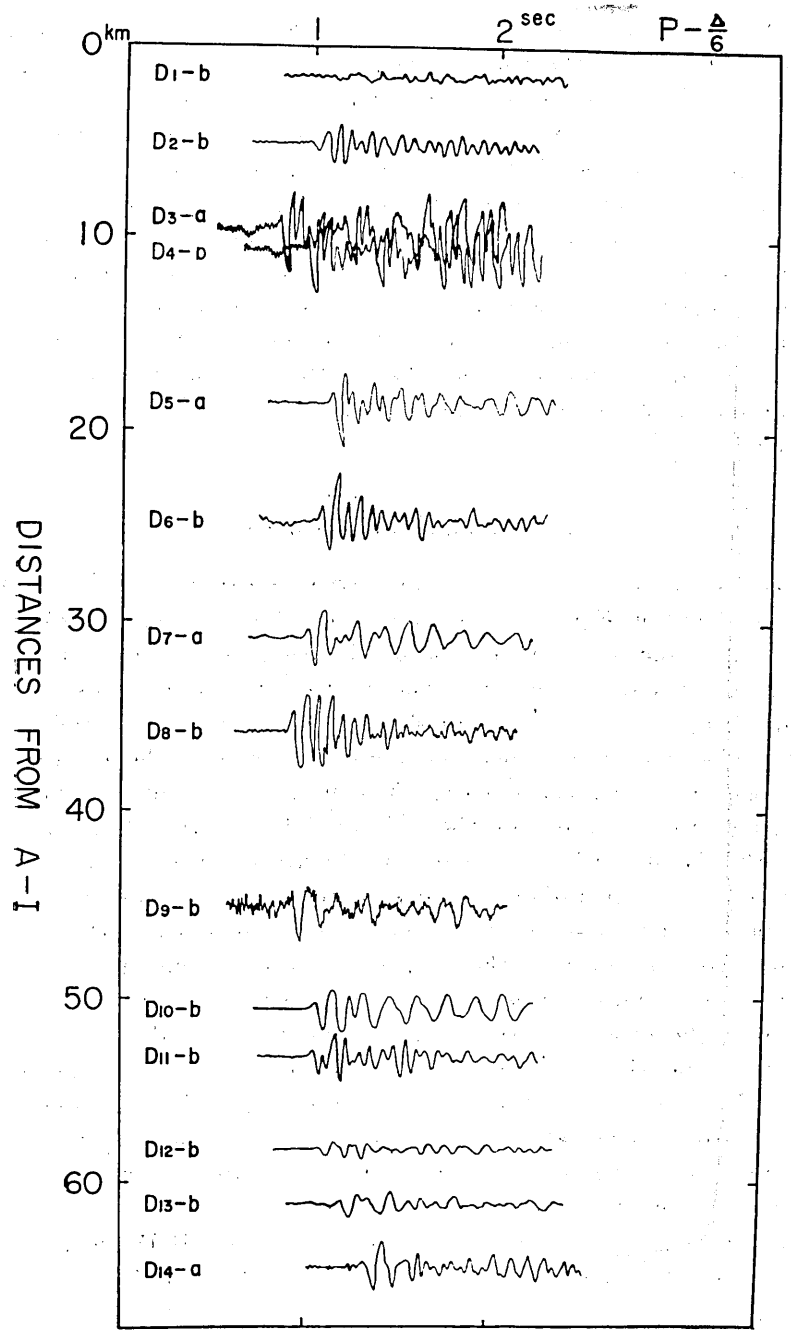

Fig. 2. Record section obtained from the fan shooting. The abscissa: $P-\Delta/6$ where Δ is the distance from shot point B-IV. The ordinate: distances for each observation site are measured from shot point A-I. The paper speed of each record is not the same, but 10 cm/s or 12.5 cm/s for most of the seismograms. Therefore, the time of the first arrival for each seismogram is fixed to the exact time of $P-\Delta/6$.

served travel time at each observation site in profile A for shot B-IV, gives the travel time from the point beneath the shot point to that beneath the observation site only through the second layer with a velocity of 6 km/s. These derived travel times are called "T_F'" in this paper.

In Fig. 3 the abscissa shows T_F' reduced with a velocity of 6.0 km/s, that is, $T_F'-\Delta/6$, where Δ is the distance between shot point B-IV and each of the respective observation sites. The ordinate in Fig. 3 is the distance of each observation site not from shot point B-IV, but from shot point A-I. Each plot has a line proportional to a kind of confidence limit, which is derived in the following way. Each arrival was identified and classified by seven seismologists into three grades (Asano *et al.*, 1969a). The extent of fluctuation in the travel time is represented by the probable error on the assumption that the observational error, the fluctua-

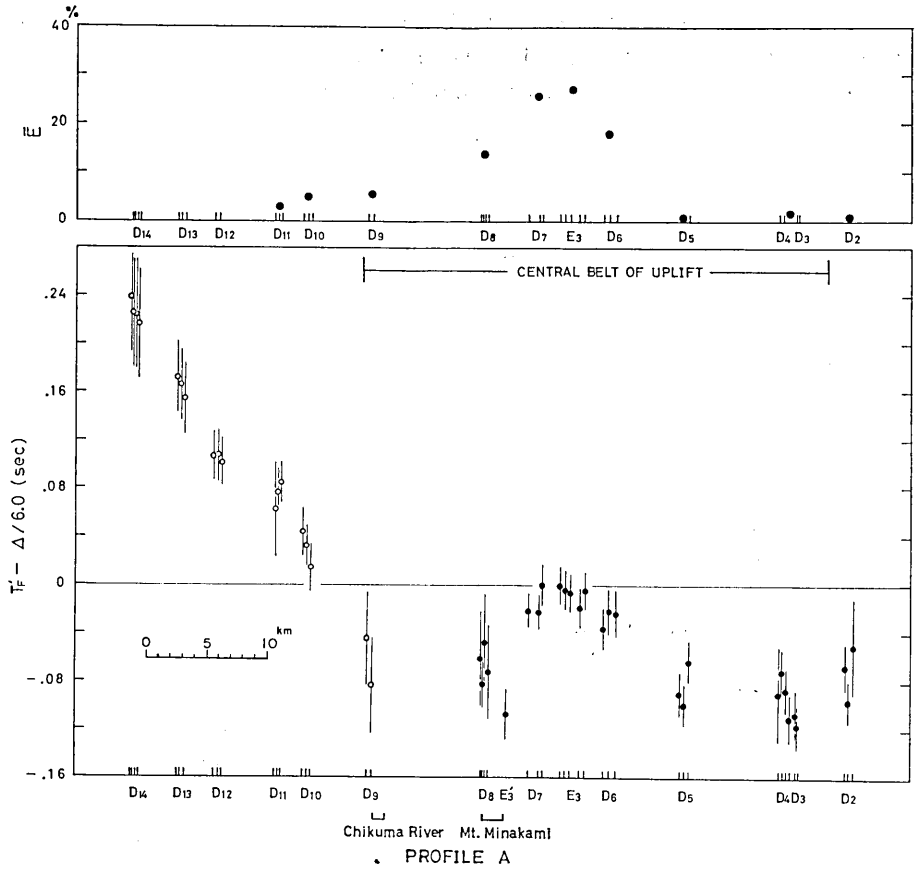

Fig. 3. Reduced T_F' graph and released seismic energy ratio $\bar{E}$ along each wave path. The abscissa shows the location of each observation site in profile A, the distance to which is measured from shot point A-I. The data at observation sites northeast of Chikuma River are shown with the closed circles and those southwest of it, with the open circles.

tion of identification, etc. satisfy the normal distribution and the time interval for each grade gives the confidence interval with a confidence coefficient of 95%. The probable error thus derived is shown by the length of line for each plot. The line in the upper part of the figure shows the observation sites, the wave path to which seems to cross the Central Belt of Uplift. In the upper figure, the released seismic energy ratio $\bar{E}$ calculated along the wave path is shown. This ratio is calculated from the formula

$$\bar{E}=\sum_i l_i \cdot E_i/\Delta, \qquad \Delta=\sum l_i$$

where E_i is the released seismic energy ratio and l_i is the length of the wave path in the region with E_i.

Fig. 3 shows the following features:

1) The "reduced T_F'" has almost the same value for the observation sites such as D_2, D_3, D_4, D_5, E_3', D_8, and D_9.
2) The "reduced T_F'" increases from D_{10} to D_{14}.

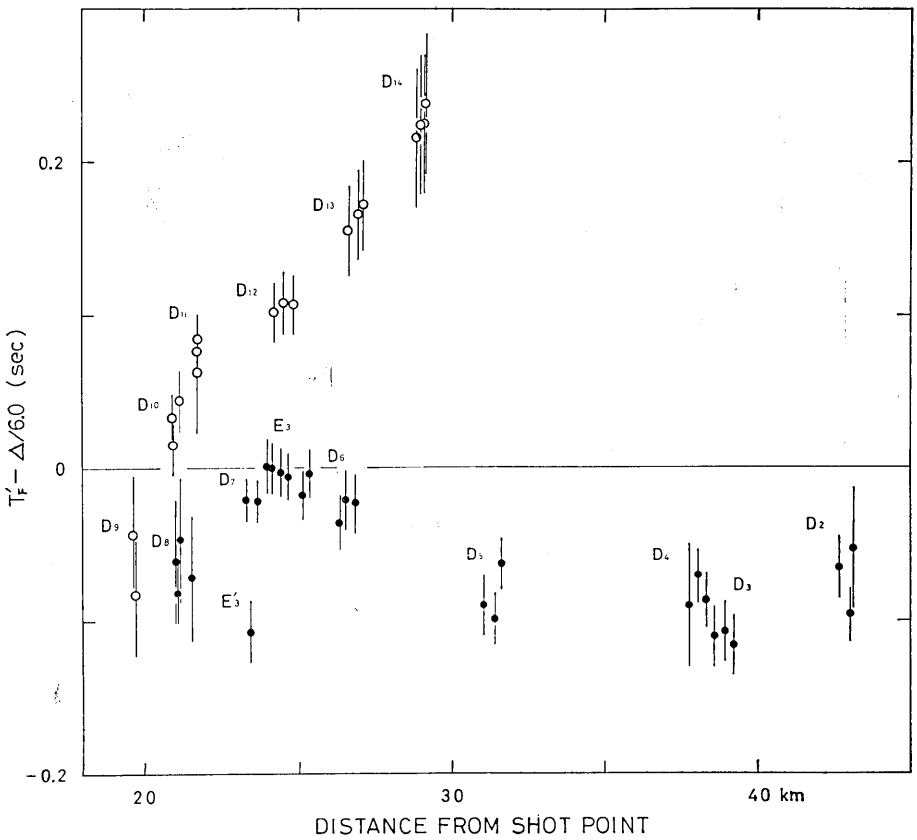

Fig. 4. Reduced T_F' graph. The abscissa is the distance from shot point B-IV.

3) The "reduced T_F'" at D_6, E_3 and D_7 is larger than at $D_2 \sim D_9$.

In Fig. 4 the "reduced T_F'" is shown with the real distance between the shot point and each observation site. The following features are observed in Fig. 4.

1) The "reduced T_F'" is almost constant at D_2, D_3, D_4, D_5, D_8 and D_9, irrespective of the distance.
2) The "reduced T_F'" increases on the farther southwestern side of D_9 as the distance from the shot point increases.
3) The "reduced T_F'" at D_6, E_3 and D_7 shows a delay due to a factor independent of the distance from the shot point in comparison with those at the other observation sites.

If the second layer in the area under consideration had a uniform velocity of 6.0 km/s as obtained in most of profile A and in profile B, the "reduced T_F'" would give a constant value—zero in the case when the assumption about the delay time is reasonable and no error of the delay time is present. From the fluctuation shown in Fig. 4, it is concluded that the second layer is not homogeneous. However, the fluctuation of the "reduced T_F'" is not at random, but depends on the azimuth of observation sites from the shot point.

4. Interval velocity

The quantity Δ/T_F' computed for each observation site is called the interval velocity, where Δ is the distance between the shot point and an observation site. Fig. 5 shows the relation between the azimuth of the observation site and the interval velocity. In this figure, the deviation of the velocity from 6.0 km/s is expressed in percents. The following points are clearly seen from this figure as expected from the features of the "reduced T_F'".

1) The interval velocity for the observation sites D_2, D_3, D_4, D_5, D_8 and D_9 is almost constant and larger than that for the other observation sites.
2) The interval velocity for the observation sites on the southwest side of Chikuma River is smaller than that on the opposite side. This tendency is in good agreement with the underground structure in profile A, which has a smaller velocity for the second layer on the southwestern portion of the profile.
3) The interval velocity for the observation sites D_6, E_3 and D_7 is smaller by about 2% than that for the other observation sites.

Although there exists a systematic change with azimuth in the interval velocity, the origin of this change can not be accurately located from only one trial of fan shooting. Generally speaking, the following three explanations are possible for the existence of regional velocity

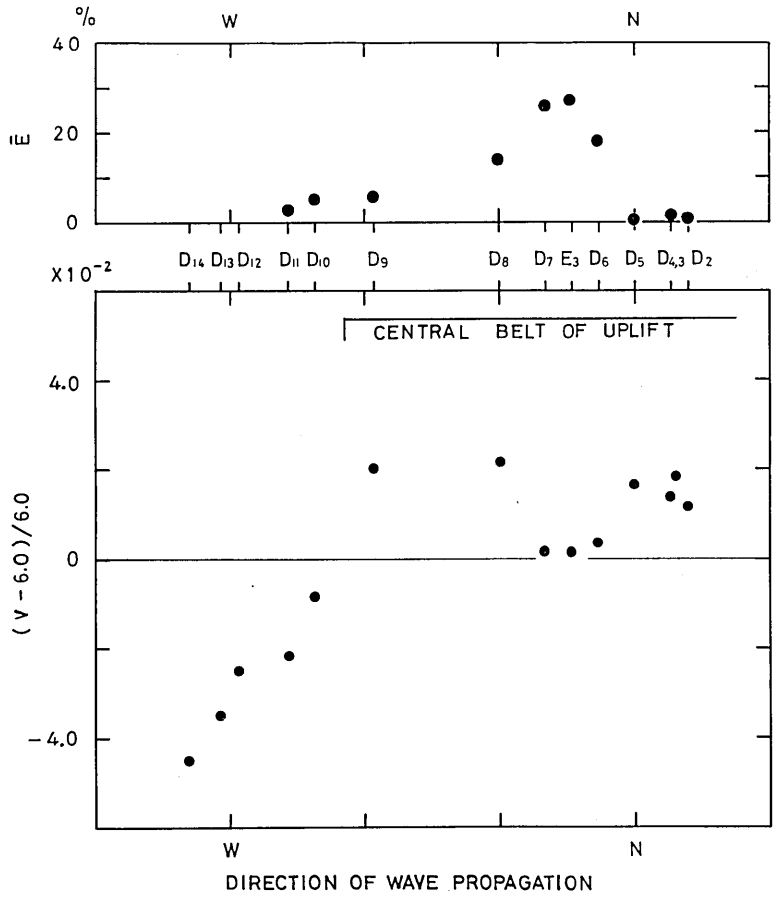

Fig. 5. Variation of the interval velocity with the direction of wave propagation. The upper figure shows the released seismic energy ratio along each wave path. The direction of wave propagation means the direction of each wave path at shot point B-IV.

variations.

1) regionality of geological features,
2) change in the physical status of hypocentral region as a result of the seismic activity,
3) abnormal physical status in the seismically active area even before the swarm earthquakes took place.

The third possibility cannot be discussed since there are no data for the time prior to the Matsushiro swarm earthquakes.

As seen from Figs. 3 and 5, the interval velocity is relatively small when the wave path crosses the area with thick sediments. That is, the interval velocity for the observation sites southwest of Chikuma River decreases toward the south linearly with respect to the azimuth from the shot point, and independently of the length of crossing the epicentral

region. This kind of decrease in the interval velocity may result probably from the first possibility. For the regionality explaining such a decrease in the interval velocity there are at least two possibilities, that is,

a) the velocity in the second layer decreases toward the south,

b) the medium with a lower velocity occupies the larger volume in the southern part so that the wave path traveling through this medium becomes longer.

However, at present it is impossible to determine which of the two really causes the decrease in the interval velocity.

It is not clear at present which of the two possibilities mentioned above are applicable to the abnormal decrease in the interval velocity at D_6, E_3 and D_7. However, as shown in Fig. 1, the wave paths to these three observation sites have larger portions in the epicentral region than those to the other observation sites. In the upper figure of Fig. 5, the released seismic energy ratio derived for each wave path, $\bar{E}$, is given. In Fig. 5 as well as in Fig. 3 there exists a good correlation between $\bar{E}$ and the interval velocity. That is, the larger the portion of wave path in the region with large released seismic energy ratio, the lower the interval velocity. But the reduced T_F' or the interval velocity at D_8 has a normal value although the wave path to D_8 has a large portion in the region with large $\bar{E}$. This might be explained with the lateral distribution of hypocenters under profile A which shows the absence of hypocenters beneath D_8 up to several km (Asano *et al.*, 1971).

5. Re-examination of travel times in profiles A and B

The good correlation between the interval velocity and $\bar{E}$ stimulates the idea that the region with decreased velocity coincides with that of hypocenters. Therefore in order to study this idea in more detail, the travel time curves in profiles A and B (Asano *et al.*, 1969b) are again examined closely especially to check whether the portion of the travel time curve corresponding to the epicentral region shows a velocity lower than the surrounding portions.

Fig. 6 shows the T' curve for the wave from the southwest to the northeast in profile A reduced with a velocity of 6.0 km/s, that is, $T'-\Delta/6$, where T' is already obtained from various combinations of shot points (Asano *et al.*, 1969b). At the top of the figure, the released seismic energy ratio is shown along profile A. There is a clear tendency in the reduced T' derived from the combination of shot points (IV-II) and (IV-I) to become larger from D_8 to E_3. These T' curves have a good accuracy since most of the seismograms obtained from these shots are of good

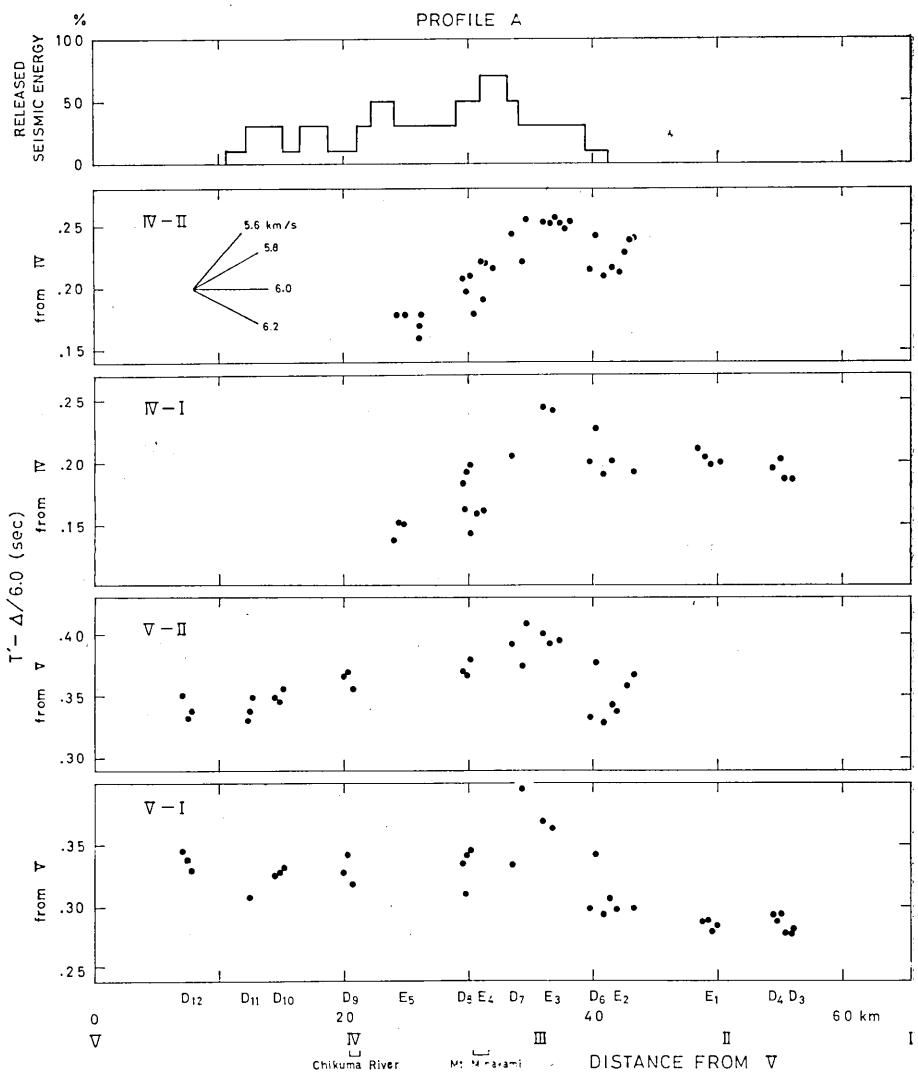

Fig. 6. Reduced T' travel time curve and released seismic energy ratio in profile A.

quality. According to the detailed studies of the T' curves by Tazime (1963), there exists a relation between the reduced T' curve and the structure as shown in Fig. 7 where v_2 is smaller than v_3. Since the tendency of $T'-\Delta/6$ from D_8 to E_3 is similar to that in Fig. 7, the existence of the material with a lower velocity in this interval is clear. The range of velocity of this lower velocity material is estimated in the figure to be 5.65~5.75 km/s by assuming this material to be homogeneous. The region with this low velocity is in good agreement with that of the largest $\bar{E}$ in the top of the figure. Although there is a slight indica-

tion that a high velocity zone exists in $E_3 \sim D_6$ adjacent to the low velocity zone in $D_8 \sim E_3$, the details are left for future studies.

Fig. 8 shows $T' - \Delta/6$ for the wave from the southeast to the northwest in profile B. Also the velocity from D_8 to E_4 is small, about 5.7 km/s. Again the region with a low velocity corresponds to that of large $\bar{E}$.

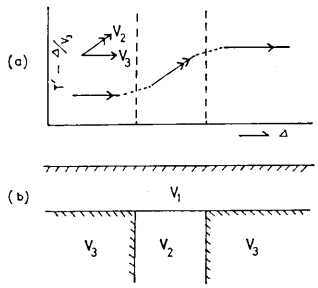

Fig. 7. Reduced T′ travel time curve (a) expected from the structure (b), where $v_3 > v_2 > v_1$. (After Tazime, 1963)

Therefore not only the results shown above but also those derived from the fan shooting method clearly show the coincidence of the low velocity region with the most seismically active one.

Now, the hypothesis is examined according to which the decrease in the interval velocity has resulted from the swarm earthquakes. The region within the contour 70% in Fig. 1 is assumed to be the region in which the decrease of velocity takes place; outside of this region the velocity is assumed to be normal, that is, 6.0 km/s. Then the velocity in this region is derived as about 5.7 km/s, by using the interval velocity. This value agrees with 5.65~5.75 km/s obtained in profile A and with 5.7 km/s in profile B. That is, the velocity derived for the seismically most active region is lower by about 5% than that for the other aseismic regions.

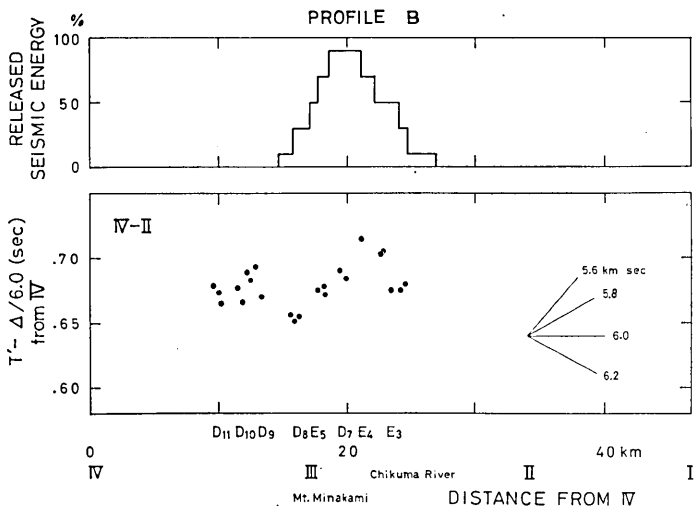

Fig. 8. Reduced T' travel time curve and released seismic energy ratio in profile B.

6. Amplitude and spectrum studies

In this paragraph the features derived from the travel time studies are examined through the amplitude and spectrum studies of the initial portion of P waves.

The amplitude of the first peak in the P wave group is measured on the good seismograms which were obtained with the instruments of good quality. In the experiment all amplifiers were calibrated twice in profile A by a special calibration team. The overall characteristics of the instruments were derived from the analysis of records of the simultaneous observation of noise and vibration due to weight dropping at one place (Asano *et al.*, 1969a). Then the measured amplitude was corrected with the magnification at 0.08 sec since the initial portion of P waves has an apparent period of about 0.08 sec. The corrected amplitude is shown in Fig. 9. In this figure, the open circles give the amplitude at the observation sites southwest of Chikuma River and the closed ones at those northeast of the river. No anomaly is present in the amplitude probably because the accuracy of amplitude measurement is insufficient as yet to detect the anomaly derived from the reduced T_F'. The line proportional to the inverse square of the distance is inserted tentatively in Fig. 9.

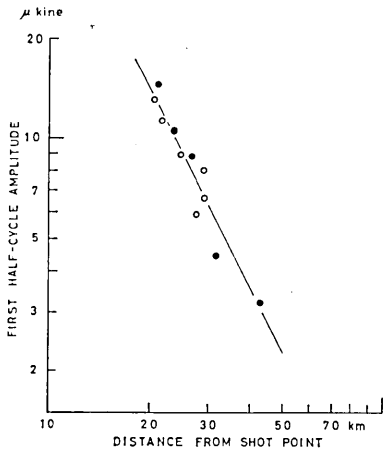

Fig. 9. Variation of velocity amplitude of the first arrival with distances from the shot point. The data at observation sites northeast of Chikuma River are shown with closed circles and those southwest of it, with open circles. The line inversely proportional to the square of the distances is inserted for reference.

Next the apparent periods of the initial portion of P waves were measured on the same seismograms as used for amplitude studies. The apparent period is defined as the time interval of 1 cycle of waves, that is, the interval between the adjacent points crossing the zero line in the same direction on the seismograms as shown in the upper part of Fig. 10. Fig. 10(a) shows the dependence of apparent frequency obtained on the azimuth of the observation sites from the shot point. D_9 near Chikuma River is the nearest observation site to the shot point. The apparent frequency becomes lower from D_9 toward the southwest depending on the distance, while on the northeastern side of Chikuma River

the apparent frequency tends to become higher as the distance increases although this tendency is not so remarkable. These tendencies are shown more clearly in Fig. 10(b). The lines in Fig. 10(b) are inserted only to show the tendency, a dotted line parallel to the solid line being shown in an arbitrary position to compare with the broken line. Also Fig. 10(b) shows the tendency that on the northeastern side of Chikuma River the rate of decrease in frequency is smaller than on the southwestern side of the river.

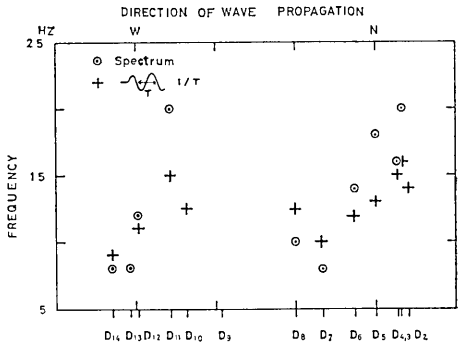

Fig. 10(a). Variation of frequency of the first arrival with directions of wave propagation.

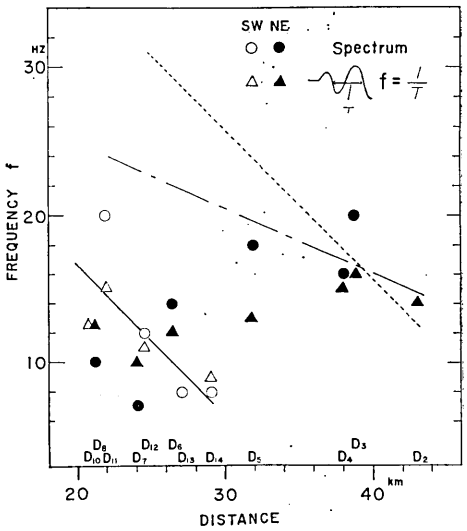

Fig. 10(b). Variation of frequency of the first arrival with distances from the shot point. The triangular marks show the apparent frequency measured from the seismograms, and the circles, the frequency giving maximum amplitude in the spectrum. The data at observation sites northeast (NE) of Chikuma River are shown with closed circles or triangles and those southwest (SW) of it, with open circles or triangles respectively. A dotted line parallel to the solid line is shown in an arbitrary position to compare with the broken line.

The spectrum of the initial portion of P waves, that is, of head waves, is calculated for detailed studies. The interval of analysis is 0.5 sec after the first arrival. The sampling rate is 100 hz and the time window $0.5(1+\cos(\pi t/T_m))$, where T_m is the sampling interval, is applied prior to the Fourier analysis. After the application of the instrumental correction, the spectrum shown in Fig. 11 is obtained.

The frequency at the maximum amplitude is taken from each figure in Fig. 11 and shown in Fig. 10(a). The tendency from these results agrees with that from the apparent frequency.

The spectrum in Fig. 11 includes not only the source spectrum but also the spectrum due to the local structures beneath the observation sites. If these characteristics could be removed, the trans-

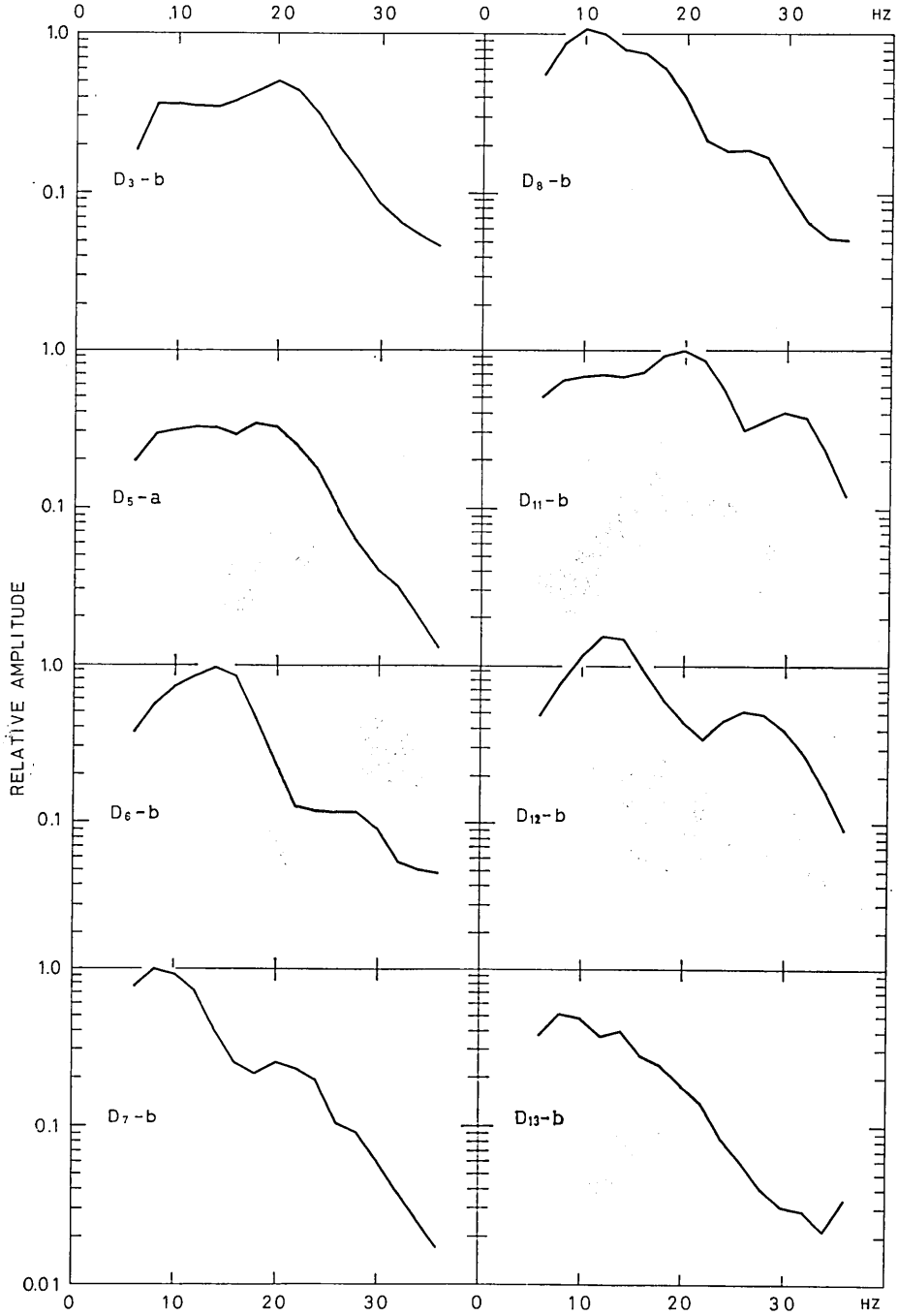

Fig. 11. Spectrum of the initial portion of waves.

fer function of the second layer with a velocity of 6.0 km/s could be obtained and absorption characteristics of this layer would be clarified. The detailed study will be published in near future, but in this paper the effect of the source spectrum was taken into account. This was done on the assumption that the spectrum obtained with the seismogram at D_{14}-b in profile B (the distance is 994 m) from shot B-IV is the same as the source spectrum. This assumption is reasonable since the structure in profile B between D_{14} and B-IV is very simple, that is, except for the very thin surface layer, the layer with a velocity of 2.4 km/s exists up to fairly large depths (Asano *et al.*, 1969b). In Fig. 12 the source spectrum thus derived is shown. Fig. 13 shows the result of the spectrum normalized at 8.0 hz after the correction of the source spectrum is applied to the spectrum of each observation site in Fig. 11. As mentioned above the spectrum in Fig. 13 includes the frequency characteristics of the local structure beneath each observation site. However, if this effect is assumed to be uniform in the frequency range 8-30 hz, the spectrum shown in Fig. 13 can be used as a transfer function of the second layer. That is, the form of each spectrum results from the frequency characteristics of the corresponding wave path. The following features are present in each spectrum of Fig. 13.

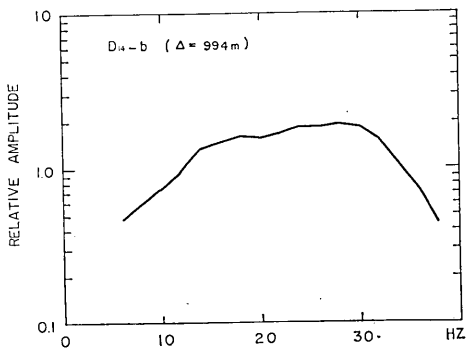

Fig. 12. Spectrum of seismic waves observed at D_{14}-b for shot B-IV, which was assumed as the source spectrum of shot B-IV in the present analysis.

(1) The gradient in the spectrum for D_6 and D_7 is the largest. It is interesting to note that the reduced T_F' and the interval velocity along the wave path to D_6 and D_7 is larger and smaller respectively than to other observation sites.

(2) The gradient in the spectrum for D_3 and D_5 is smaller than for other observation sites. The interval velocity to D_3 and D_5 is relatively large.

(3) The gradient in the spectrum for D_{13} is fairly large. There is an indication of a change in the local structure near D_{13}, i.e. the surface structure changes on the southwestern side of D_{13} and the velocity in the surface layer becomes small. Therefore, the frequency characteristics at D_{13} might be different from those at other observation sites.

Now, the average attenuation factor Q is derived from the dotted

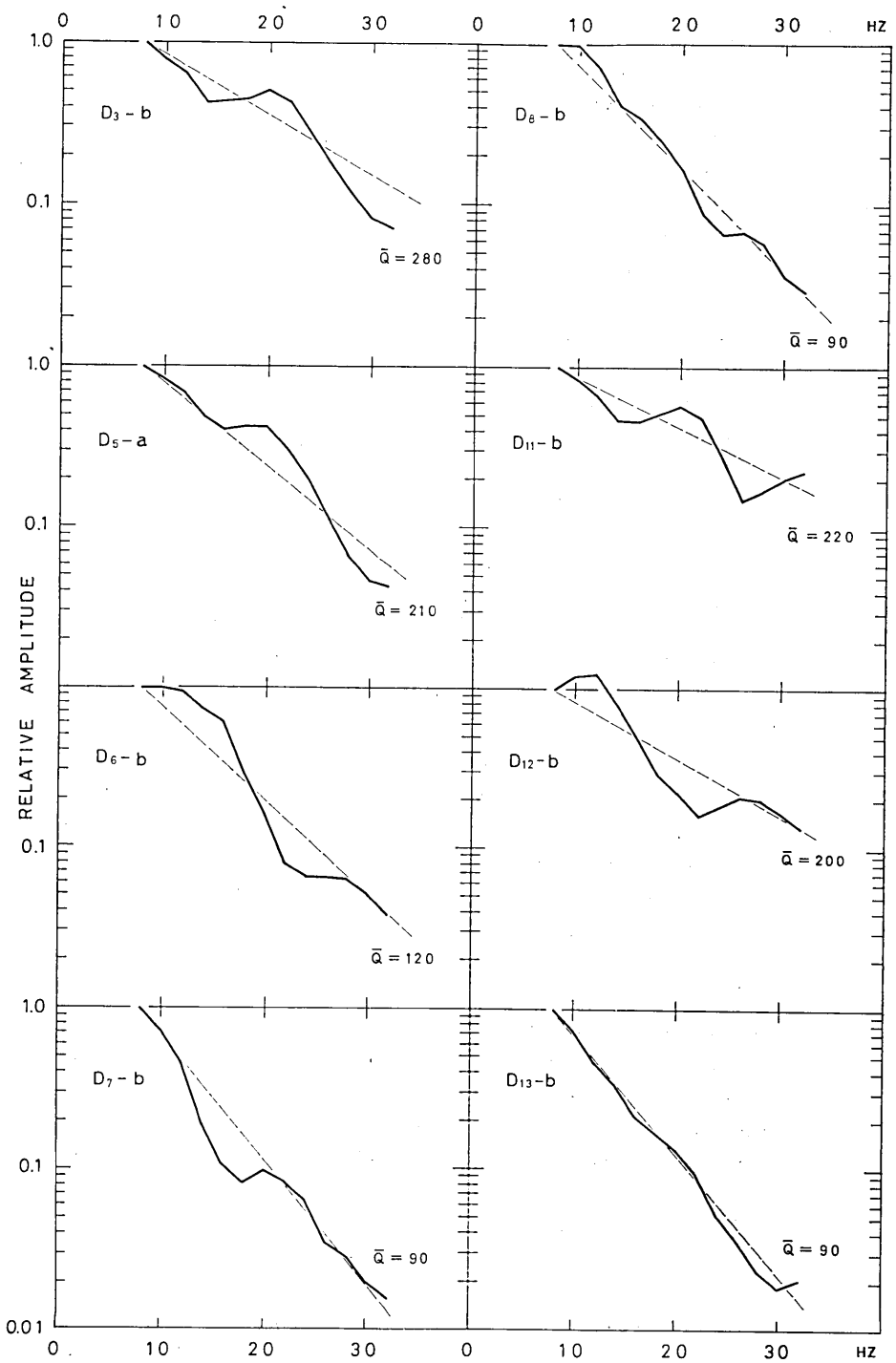

Fig. 13. Spectrum and attenuation factor derived. Each spectrum is normalized at 8.0 hz after the correction of the source spectrum (Fig. 12) is applied to the spectra in Fig. 11.

line in Fig. 13 fitted to the spectrum in the range 8-30 hz by the formula $\alpha=\pi\tau/Q$ where α is the gradient of the dotted line and τ is the travel time. For this procedure the Q value is assumed to be independent of frequency. The Q value thus obtained is shown in Fig. 14, where the abscissa is the azimuth of each wave path measured from the shot point. The range of Q values obtained is 100-300, which is lower than the value generally expected for the crust. This small value is considered to be due to the effect of the small value in the superficial layers.[1] Fig. 14 shows that the Q value in the region with a small interval velocity is relatively small. That is, the analysis of seismograms obtained by the fan shooting technique shows that there exists a good correlation between the small interval velocity and the small Q value.

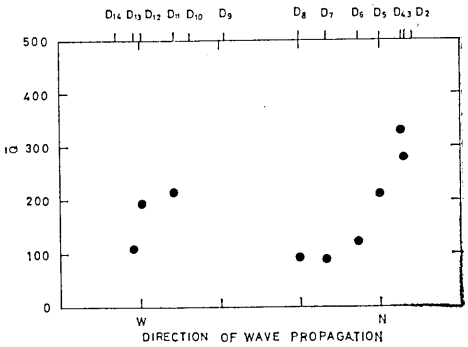

Fig. 14. Variation of the attenuation factor with the directions of wave propagation.

7. Discussions and Conclusions

From the studies mentioned above the existence of an anomaly in the second layer within the hatched region of Fig. 15 becomes clear. That is, in the hatched region there exist materials with different physical properties, i.e., low interval velocities and large attenuation, from those in the other regions. Also along profiles A and B there are regions with a relatively low velocity as shown doubly hatched in Fig. 15. The location of the region with a low velocity and a large attenuation coincides with that of the seismically most active region. The velocity is lower by about 5% and the Q value is smaller by 50% in this anomalous region if compared with the surrounding regions.

It is fairly difficult to explain what is the real relation between the anomalous structure and the seismic activity, although the anomaly of structure in the seismically most active region was derived with certainty. Whether the anomalous structure results from the seismic activity or whether it has been present there before the swarm earth-

1) Recently S. Suzuki obtained the value of about 1000 for the average Q value in profile A after eliminating the effect of superficial layers. Read at the annual meeting of the Seismological Society of Japan on May 13, 1970.

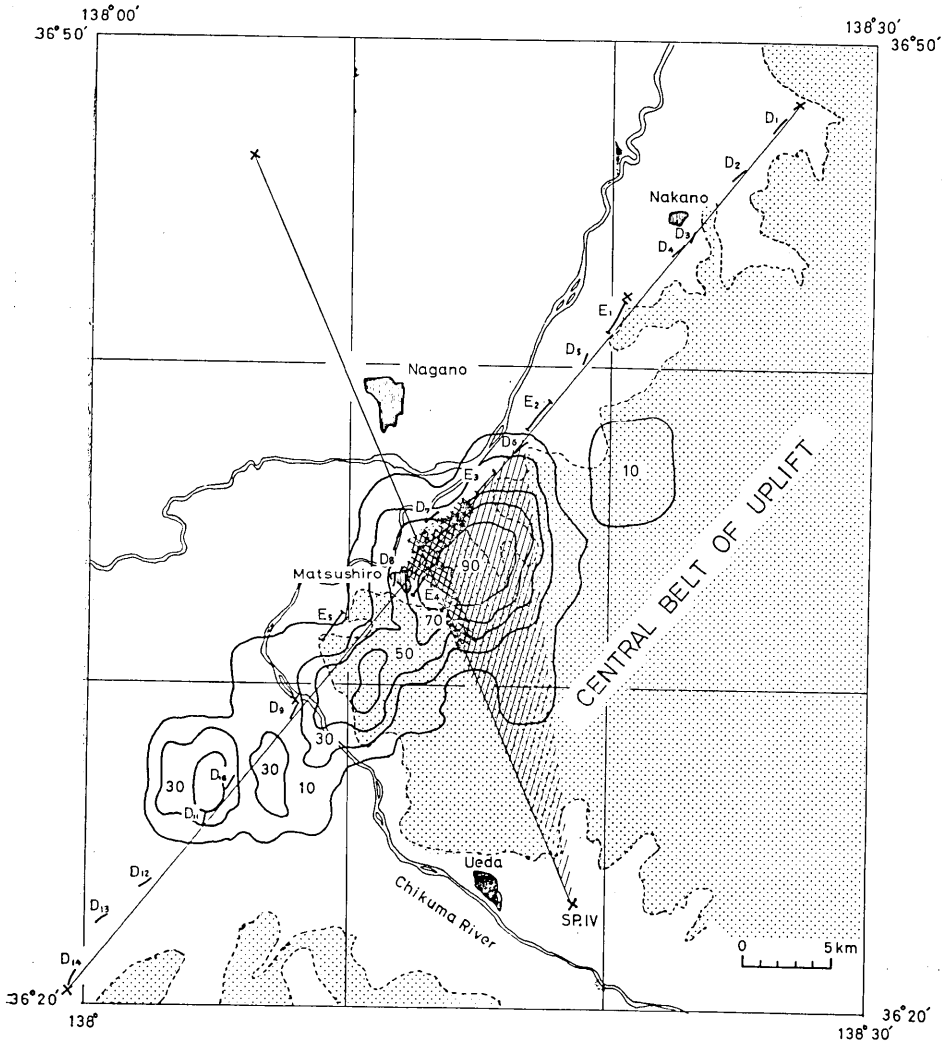

Fig. 15. Location of anomalous structures derived through the present analysis.
Hatched area: the area with an anomalous structure from the fan shooting.
Doubly hatched area: the area with an anomalous structure in profile A or in profile B
Contour: released seismic energy ratio. Numbers indicate released seismic energy ratio in %.
The Central Belt of Uplift is roughly shown with small dots.

quakes, being rather the cause of seismic activity, can not be answered definitely yet. There are no data for the latter possibility, while there are little data for the former possibility although they are not so direct and powerful. Kasahara *et al.* (1966a, 1966b, 1967) studied the relation between the strain energy and the seismic energy in the Matsushiro earthquake swarm area with the electro-optical geodetic measurement.

They emphasized that about one year after the swarm earthquakes, i.e. in the period about one year prior to the present experiment, a non elastic deformation occurred. In their opinion, the fracture played an important role in this non elastic deformation. If so, the assumption μ=constant which was adopted for the computation of strain energy does not hold any longer. This change in the rigidity gives one of the possibilities to lower the velocity.

S. Suyehiro (1968) reported that there exists a change in the spectrum of seismic waves observed before and after the swarm earthquakes occurred. According to his results, the high frequency component was rich for the seismic waves crossing the epicentral region before the seismicity became active, while the high frequency component was poor after the main seismic activity had almost finished. This result supports the possibility that the large attenuation of seismic waves in the hypocentral region results from the strong seismic activity.

The phenomena of landslides, anomalous welling of water (Morimoto *et al.*, 1967) and abnormal change in the horizontal strain (Kasahara *et al.*, 1966a, 1966b, 1967) took place in the region involved in the hatched part of Fig. 15.

Acknowledgement

The data used in this paper were obtained from a cooperative experiment. We want to express our hearty gratitude to the scientists and the technicians who participated in this experiment. The travel time given in Table 1 was derived by Dr. H. Watanabe, Messrs. K. Ichikawa, M. Nogoshi, S. Kubota and H. Suzuki in addition to two of the present authors. We are also grateful to them. Also we are much obliged to Miss Y. Okuda for assistance in preparing figures and manuscripts.

References

ASANO, S., K. ICHIKAWA, H. OKADA, S. KUBOTA, H. SUZUKI, M. NOGOSHI, H. WATANABE, K. SEYA, K. NORITOMI, and K. TAZIME, 1969a. Explosion seismic observations in the Matsushiro Earthquake Swarm Area, *Sp. Rep. Geol. Survey of Japan*, No. **5**, 1-162.

ASANO, S., S. KUBOTA, H. OKADA, M. NOGOSHI, H. SUZUKI, K. ICHIKAWA, and H. WATANABE, 1969b. Underground structure in the Matsushiro Earthquake Swarm Area as derived from explosion seismic data, *Sp. Rep. Geol. Survey of Japan*, No. **5**, 163-203.

ASANO, S., S. KUBOTA, and H. OKADA, 1971. Crustal structure and distribution of hypocenters in the Matsushiro Earthquake Swarm Area, *Bull. Earthq. Res. Inst.*, in preparation.

HAGIWARA, T., and T. IWATA, 1968. Summary of the seismographic observation of Matsushiro Swarm Earthquakes, *Bull. Earthq. Res. Inst.*, **46**, 485-515.

HAGIWARA, T., J. YAMADA, and M. HIRAI, 1966. Observation of tilting of the earth's surface due to Matsushiro Earthquakes, Part I, *Bull. Earthq. Res. Inst.*, **44**, 351-361.

ICHIKAWA, M., 1969. Matsushiro earthquake swarm, *Geophys. Mag.*, **34**, 307-331.

KASAHARA, K., and A. OKADA, 1966a. Electro-optical measurement of horizontal strains accumulating in the swarm earthquake area (1), *Bull. Earthq. Res. Inst.*, **44**, 335-350.

KASAHARA, K., A. OKADA, M. SHIBANO, K. SASAKI, and S. MATSUMOTO, 1966b. Electro-optical measurement of horizontal strains accumulating in the swarm earthquake area (2), *Bull. Earthq. Res. Inst.*, **44**, 1715-1733.

KASAHARA, K., A. OKADA, M. SHIBANO, K. SASAKI, and S. MATSUMOTO, 1967. Electro-optical measurement of horizontal strains accumulating in the swarm earthquake area (3), *Bull. Earthq. Res. Inst.*, **45**, 225-239.

MORIMOTO, R., K. NAKAMURA, Y. TSUNEISHI, J. OSSAKA, and N. TSUNODA, 1967. Landslides in the epicentral area of the Matsushiro Earthquake Swarm—their relation to the earthquake fault, *Bull. Earthq. Res. Inst.*, **45**, 241-263.

Nagano-ken Chigakukai (Geological Association of Nagano Prefecture), 1962. Geological Map of Nagano Prefecture, *Naigai Map Company*.

NAKAMURA, K., and Y. TSUNEISHI, 1967. Ground cracks at Matsushiro probably of underlying strike-slip fault origin, II. The Matsushiro Earthquake Fault, *Bull. Earthq. Res. Inst.*, **45**, 417-471.

SUYEHIRO, S., 1968. Change in earthquake spectrum before and after the Matsushiro Swarm, *Pap. Met. Geophys.*, **19**, 427-435.

TAZIME, K., 1963. Refraction shooting on the experimental field for small explosions in the neighbourhood of the City of Mitsuke, Niigata Prefecture, *Geophys. Bull. Hokkaido Univ.*, **11**, 113-168.

TSUBOKAWA, I., A. OKADA, H. TAJIMA, I. MURATA, K. NAGASAWA, S. IZUTSUYA, and Y. ITO, 1967. Levelling resurvey associated with the area of Matsushiro Earthquake Swarms. (1), *Bull. Earthq. Res. Inst.*, **45**, 265-288.

---

44. Fan shooting により得られた松代群発地震域における地下構造異常

北海道大学理学部 岡田 広 / 鈴木貞臣
東京大学地震研究所 浅野周三

1967 年 11 月～12月，松代群発地震域の地下構造の爆破地震学的調査が A，B 2 測線において行われた．得られた地下構造は種々の調査結果の理解に資し，松代群発地震の研究に貴重な資料を提供した．この調査の際，地下構造異常を見出す目的で A 測線の観測点に対して，B-IV において爆破を実施した．これは 1 種の Fan shooting であるが，この程度の規模の，複雑な地質を有する地域で，この方法がどの程度有効かという点にも興味があった．A, B 両測線において 6 km/s 層以浅の構造がかなり詳細に得られており，この知識を用いることによって，地震活動が最もはげしかった地域を通る P 波の平均速度が 2%，他の地域を通るもののそれより小さいことがわかった．また，この減少の原因が最も地震活動がはげしかった地域のみに存在するとすると，5.7 km/s となり約 5% 小さいことになる．A, B 両測線でも速度の小さい地域が地震活動の大きかった所に存在し，その値は，やはり 5.65—5.75 km/s となり一致は著しい．また，千曲川の南西側の観測点では速度が系統的に距離とともにおそくなる傾向が存在する．さらに初動部分の見掛振動数，スペクトルの最大振幅を与える振動数の何れもが，異常を示した地域では周囲に比較して低い．かくして，ある程度調査地域

が広くて複雑でも，主測線に適当に精密な観測資料があれば Fan shooting によって異常構造を推定し得ることが確かめられた．しかし，1回のみの Fan shooting によっては，このように確かめられた松代地域の地下構造異常が地震の結果なのか，あるいは，群発地震が起る以前から存在していて地震の発生に関係があるかを実証するには十分でなく，次の機会を待たねばならない．